Adsorption of Chromium on Activated Carbon: Experimental and Modeling studies

SULF

A thesis submitted in Partial Fulfillment of the Requirements for the Degree of

Master of Technology

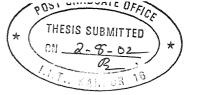
by

Suresh Gupta



to the
Department of Chemical Engineering
Indian Institute of Technology Kanpur.

August, 2002



CERTIFICATE

It is certified that the work contained in the thesis entitled Adsorption of Chromium on Activated Carbon: Experimental and Modeling Studies by Suresh Gupta has been carried out under my supervision and that this work has not been submitted elsewhere for a degree.

August, 2002

Dr. Goutam Deo

Associate Professor

Department of Chemical Engineering

Indian Institute of Technology Kanpur

4 FEB 2003 / CHE कुम्बोत्य कार्यान्य कार्यान्य प्रतकालय भारतीय प्रीयोगिकी संस्थान कानपुर अवाध्ति कः A 141901



Dedicated

To

My Parents

Acknowledgements

I express my profound sense of gratitude to my thesis supervisor **Dr. Goutam Deo** for his invaluable guidance, constructive suggestions, constant encouragement and a lot of patience throughout my M.Tech project. Without his help and encouragement this work would not have been possible.

I would also like to thank Prof. A. B. L. Agarwal and Dr. A. Bhowal for their valuable guidance.

I would also like to thank Prof. P. K. Bhattacharya for allowing me to use their lab resources.

I would also like to thank my labmates Maymol, Sravan, Rohit, Mahendra, Kamala, and Laxman for their cooperation, Dharmendra and Hemant (lab assistant) for helping me to arrange the resources.

I wish to extend my special thanks to all my friends, Swatantra, Gourav, Rajeev, Kanu, Tirtha, Vishal, Neeraj, Negi, Sushil, Partho, Prakash, Saurabh, Satish, Verma, Palival, Gargi, and Amit for their memorable company throughout my stay at IIT/K.

Finally, I would like to thank all my family members for their love, help and encouragement in each and every moment.

Suresh Gupta

Contents

List of Figures		vii	
List of Tables List of Symbols		x	
		xii	
Ab	Abstract		xiii
Ch	apters		
1.	Introduct	tion	1
	1.1 Introd	uction	1
	1.2 Object	tive	3
2.	Literatur	e Review	4
	2.1 Gener	al	4
	2.2 Source	ces of chromium	4
	2.3 Effect	s of chromium	5
	2.4 Metho	ods of chromium(VI) ion Removal from Water	6
	2.4.1	Reduction and Precipitation Method	7
	2.4.2	Ion Exchange Method	7
	2.4.3	Electrodialysis	8
	2.4.4	Electrochemical Precipitation	8
	2.4.5	Adsorption Method	9
	2.4	4.5.1 Activated Alumina Adsorption	9
	2.4	4.5.2 Activated Carbon Adsorption	9
3.	Materials	s and Methods	11
	3.1 Mater	ials	11
	3.1.1	Activated carbon and Activated alumina	11
	3.1.2	Chromium(VI) solution	12
	3.2 Metho	od of Analysis	12
	3.3 Exper	iments	13
	3.3.1	Batch Experiments	13
	3.3.2	Continuous Experiments	13
	3.3.3	Regeneration	15
4.	Modeling	•	17

	4.1 Modeling Approach	17
	4.2 Material balance relationship for fixed-bed adsorption process	19
	4.3 Lumped parameter model	20
5.	Results	27
	5.1 Batch Studies	27
	5.2 Continuous Studies	28
	5.3 Modeling Studies	30
6.	Conclusions And Suggestions for Future Studies	48
	6.1 Conclusions	48
	6.2 Suggestions for future studies	49
Re	ferences	50
Ap	pendix A Tabular Results of Batch and Continuous Experiments	54
Ap	pendix B Model Parameters and constants	64
Δn	mendix C Code in C Language for the Model	65

List of Figures

	Page No.
Fixed-bed experimental setup for continuous experiments.	16
Elemental segments in a packed-bed, column adsorption	
contactor	21
Flow chart for the lumped parameter model	26
Adsorption isotherm for chromium (VI) and activated carbon	
system.	34
Adsorption isotherm for chromium (VI) and activated alumina	
system.	35
Effect of flow rate on dimensionless chromium(VI) ion	
concentration. Mass of activated carbon = 15 g, inlet	
chromium(VI) ion concentration = 100 mg/l and	
particle size = 0.115 cm.	36
Effect of mass of activated carbon on dimensionless effluent	
chromium (VI) concentration. Inlet chromium(VI) ion	
concentration = 50 mg/l, flow rate = 15 ml/min, and particle	
size = 0.115 cm.	37
Effect of chromium(VI) ion concentration on dimensionless	
effluent chromium(VI) ion concentration. Mass of activated	
carbon = 15 g, flow rate = 15 ml/min, and particle	
size = 0.115 cm.	38
Effect of particle size on dimensionless effluent chromium(VI)	
ion concentration. Inlet chromium(VI) ion	
concentration = 100 mg/l, flow rate = 15 ml/min, and mass of	
activated carbon = 15 g.	39
Effect of regeneration of activated carbon (AC) on dimensionle	SS
effluent chromium(VI) ion concentration. Inlet chromium(VI)	
ion concentration = 100 mg/l, flow rate = 5 ml/min, mass of	
activated carbon = 15 g, and particle size = 0.115 cm.	40
	Elemental segments in a packed-bed, column adsorption contactor Flow chart for the lumped parameter model Adsorption isotherm for chromium (VI) and activated carbon system. Adsorption isotherm for chromium (VI) and activated alumina system. Effect of flow rate on dimensionless chromium(VI) ion concentration. Mass of activated carbon = 15 g, inlet chromium(VI) ion concentration = 100 mg/l and particle size = 0.115 cm. Effect of mass of activated carbon on dimensionless effluent chromium (VI) concentration. Inlet chromium(VI) ion concentration = 50 mg/l, flow rate = 15 ml/min, and particle size = 0.115 cm. Effect of chromium(VI) ion concentration on dimensionless effluent chromium(VI) ion concentration. Mass of activated carbon = 15 g, flow rate = 15 ml/min, and particle size = 0.115 cm. Effect of particle size on dimensionless effluent chromium(VI) ion concentration. Inlet chromium(VI) ion concentration = 100 mg/l, flow rate = 15 ml/min, and mass of activated carbon = 15 g. Effect of regeneration of activated carbon (AC) on dimensionle effluent chromium(VI) ion concentration. Inlet chromium(VI)

Fig 5.8	Comparison of external transport model with experimental	
	results. Mass of activated carbon = 15 g, inlet chromium(VI)	
	ion concentration = 100 mg/l, flow rate = 15 ml/min, particle	
	size = 0.115 cm, and apparent inlet chromium(VI) ion	
	concentration $(C_0^a) = 72 \text{ mg/l}$	41
Fig 5.9	Comparison of external transport model with experimental	
	results. Mass of activated carbon = 15 g, inlet chromium(VI)	
	ion concentration = 100 mg/l, flow rate = 10 ml/min, particle	
	size = 0.115 cm, and apparent inlet chromium(VI) ion	
	concentration $(C_0^a) = 68 \text{ mg/l}$	42
Fig 5.10	Comparison of external transport model with experimental	
	results. Mass of activated carbon = 15 g, inlet chromium(VI)	
	ion concentration = 100 mg/l, flow rate = 5 ml/min, particle	
	size = 0.115 cm, and apparent inlet chromium(VI) ion	
	concentration $(C_0^a) = 62 \text{ mg/l}$	43
Fig 5.11	Comparison of external transport model with experimental	
	results. Mass of activated carbon = 15 g, inlet chromium(VI)	
	ion concentration = 50 mg/l, flow rate = 15 ml/min, particle	
	size = 0.115 cm, and apparent inlet chromium(VI) ion	
	concentration $(C_0^a) = 32 \text{ mg/l}$	44
Fig 5.12	Comparison of external transport model with experimental	
	results. Mass of activated carbon = 10 g, inlet chromium(VI)	
	ion concentration = 50 mg/l, flow rate = 15 ml/min, particle	
	size = 0.115 cm, and apparent inlet chromium(VI) ion	
	concentration $(C_0^a) = 35 \text{ mg/l}$	45
Fig 5.13	Comparison of external transport model with experimental	
	results. Mass of activated carbon = 15 g, inlet chromium(VI)	
	ion concentration = 100 mg/l, flow rate = 15 ml/min, particle	
	size = 0.045 cm, and apparent inlet chromium(VI) ion	
	concentration $(C_0^a) = 72 \text{ mg/l}$	46

Fig 5.14 Comparison of external transport model with experimental results. Mass of activated carbon = 15 g, inlet chromium(VI) ion concentration = 100 mg/l, flow rate = 15 ml/min, particle size = 0.198 cm, apparent inlet chromium(VI) ion concentration $(C_0^a) = 72 \text{ mg/l}$ 47

List of Tables

		Page No.
Table 2.1	General properties of activated carbon.	11
Table 2.2	General properties of activated alumina	12
Table 5.1	Standard deviation calculations for external transport model	
	for $n = 20$.	33
Table A1	Batch experiment results for adsorption isotherm of	
	chromium(VI) and activated carbon system.	54
Table A2	Batch experiment results for adsorption isotherm of	
	chromium(VI) and activated alumina system.	55
Table A3	Continuous experiment results for mass of activated carbon	
	= 15 g, inlet chromium (VI) concentration = 100 mg/l, flow	
	rate = 15 ml/min, and particle size = 0.115 cm.	56
Table A4	Continuous experiment results for mass of activated carbon	
	= 15 g, inlet chromium (VI) concentration = 100 mg/l, flow	
	rate =10 ml/min, and particle size = 0.115 cm.	57
Table A5	Continuous experiment results for mass of activated carbon	
	= 15 g, inlet chromium (VI) concentration = 100 mg/l, flow	
	rate = 5 ml/min, and particle size = 0.115 cm.	58
Table A6	Continuous experiment results for mass of activated carbon	
	= 15 g, inlet chromium (VI) concentration = 50 mg/l, flow	
	rate = 15 ml/min, and particle size = 0.115 cm.	59
Table A7	Continuous experiment results for mass of activated carbon	
	= 10 g, inlet chromium (VI) concentration = 50 mg/l, flow	
	rate = 15 ml/min, and particle size = 0.115 cm.	60
Table A8	Continuous experiment results for mass of regenerated	
	activated carbon = 15 g, inlet chromium (VI)	
	concentration = 100 mg/l, flow rate = 15 ml/min,	
	and particle size = 0.115 cm.	61
Table A9	Continuous experiment results for mass of activated carbon	
	= 15 g inlet chromium (VI) concentration = 100 mg/l, flow	

	rate = 15 ml/min, and particle size = 0.0445 cm.	62
Table A10	Continuous experiment results for mass of activated	
	carbon = 15 g, inlet chromium (VI) concentration = 100 mg/l,	
	flow rate = 15 ml/min, and particle size = 0.1975 cm.	63

List of Symbols

U	Volumetric flow rate of water, cm ³ /sec	
C	Solution phase chromium(VI) ion concentration, g/cm ³	
q	Solid phase fluoride ion concentration, g/g adsorbent	
Z	Axial distance, cm	
t	Elapsed time in, sec	
A	Cross-sectional area of column, cm ²	
3	Porosity of the packed bed, dimensionless	
ρ	bed density in, g/cm ³	
V	Volume of each element, cm ³	
n	Number of elements in the bed	
R_{An}	Rate of adsorption for the nth element, g chromium(VI) ion/g adsorbent/sec	
K_{P}	Mass transfer coefficient (pore), cm/sec	
A_s	External interfacial transfer area for adsorbent, cm ² /cm ³	
A_p	Surface area of pores, cm ² /cm ³	
C*	Solution phase chromium(VI) ion concentration considered to be in equilibrium	
	with the outer surface of the adsorbent particle, g/cm ³	
D_{pore}	Diffusivity of chromium(VI) ion in the pore of adsorbent particle, cm ² /sec	
X	Internal porosity of adsorbent particles, dimensionless	
D_1	Diffusivity of chromium(VI) ion in water, cm ² /sec	
$K_{\mathbf{f}}$	Film-diffusion controlled mass transfer coefficient, cm/sec	
ja	Mass transfer factor, dimensionless	
N_{Re}	Reynolds number, dimensionless	
K	Over-all mass transfer coefficient, cm/sec	
\mathbf{C}_0	Inlet fluoride ion concentration, mg/l	
υ	Kinematic viscosity of water, cm ² /sec	
$\mathbf{D}_{\mathtt{P}}$	Average diameter of adsorbent particle in, cm	
D	Diameter of column in, cm	
Н	Bed height of activated carbon, cm	

Abstract

Experimental and modeling studies for continuous fixed-bed adsorption are considered for the removal of chromium(VI) from water. Experimental studies involved batch and continuous fixed-bed experiments. Batch experiments are conducted for two adsorbents, activated carbon and activated alumina. From the batch experiments results it is observed that the adsorption isotherm for both adsorbents are essentially Langmurian in nature. Furthermore, the adsorption capacity of activated carbon is higher than the activated alumina used in the present study. Langmuir constants, a and b, for the chromium(VI)activated carbon system were 0.178 and 0.010 and for the chromium(VI)-activated alumina system were 0.028 and 0.003. Continuous experiments were carried out in a fixed-bed column and the conditions varied were flow rate, mass of activated carbon, inlet chromium(VI) ion concentration, and particle size. The adsorption curves obtained essentially had three distinct regions. Initially, the oulet concentration of chromium(VI) was negligible. Thereafter, the outlet concentration increased rapidly till an apparent concentration C_0^a , which was about 0.6 to 0.75 of the actual outlet concentration, C_0 . Finally, after reach the apparent C_0^a value, the outlet concentration increases gradually. Continuous experiment were also conducted for regenerated activated carbon. Regeneration of activated carbon was done by alkali-acid treatment. Even after several alkali-acid treatment cycles the original adsorption curve was not obtained. Modeling of the adsorption phenomena was achieved by considering a Lumped parameter model. In this model the partial-differential material-balance equations are converted into ordinary differential equations. The model is able to represent the experimental results reasonably well based on external transport being limiting and a constant value for the diffusivity of $4.31*10^{-5}$ cm²/s.

CHAPTER 1

1.1 Introduction

The availability of water supply adequate in terms of both quantity and quality is essential to human existence. The importance of water was recognized early and civilization developed around water bodies that could support agriculture, transportation, and provide drinking water. As human activity increased the amount of pollutants entering into water streams also increased. Usually smaller streams are affected first and then larger streams and lakes become polluted. For controlling the water pollution, pollution control programs have been initiated in several countries to reduce the contaminants discharged to these water streams and ground water (Peavy, 1988).

All metals are soluble to some extent in water (Metcalf and Eddy, 1995). Trace quantities of many metals, such as, nickel, lead, chromium, cadmium, zinc, copper, iron and mercury are important constituents of most waters. Some of these metals are necessary for growth of biological life and absence of sufficient quantities of them could limit growth, for example, of algae (Metcalf and Eddy, 1995). The presence of any of these metals in excessive quantities will, however, interfere with many beneficial uses of water due to their toxicity. Therefore, it is frequently desirable to measure and control the concentrations of these substances in water.

Chromium is an important metal for some industries, such as, electroplating, leather tanning, paints, and pigments etc (Sharma, 2001; Low et al., 1997) and has the potential to contaminate drinking water sources. Chromium exist in different oxidation states in nature of which chromium(VI) is the most water soluble and easily enters living cells. Chromium(VI) is a human carcinogen, as determined by the National Toxicology

Program (NTP), the International Agency for Research on Cancer (IARC), the U.S. Environmental Protection Agency (U.S. EPA), and OEHHA (IARC, 1990; U.S. EPA, 1998b; Siegel, 1990). Furthermore, OEHHA has made a health protective assumption that chromium(VI) is a potential human carcinogen by the oral route (Siegel, 1990). Chromium(III) on the other hand has not been shown to be carcinogenic to animals or humans by the oral route (IARC, 1990; U.S. EPA, 1998a; ATSDR, 1993 and 1998).

Various technologies available for the treatment of chromium(VI) rich wastewaters include ion-exchange, solvent extraction, chemical precipitation etc (Mukherjee, 1986). These methods are, however, cost intensive and are unaffordable for large scale treatment of wastewater rich in chromium(VI) for developing nations.

Adsorption is an effective method for the treatment of industrial effluents and quite popular in developed countries. Activated carbon and activated alumina has been widely used as an effective adsorbent for the removal of many aqueous organic and inorganic contaminants (Han et al., 2000). Large specific surface area and presence of different surface functional groups (e.g., oxygen-containing groups such as hydroxyl, carbonyl, lactone, and carboxylic acids) are well-known characteristics of activated carbons that make them excellent adsorbents (Corapcioglu and Huang, 1987; Sontheimer et al., 1988). Activated alumina is one of the solids having the greatest affinity for water. An important industrial application for activated alumina is adsorption of solute from the waste water because of its large surface area (Yang, 1999). The use of activated carbon for chromium removal has been studied by several researchers (Nagasaki, 1974; Miyagawa et al., 1976; Huang and Wu, 1975; Ouki and Neufeld, 1997). These studies, however, did not involve modeling of continuous fixed-bed experiments. Recently

(Gupta et al., 2002), have used a simplistic model for effectively describing the continuous fixed-bed experiments for fluorine adsorption. It is the aim of the present study to test the validity of the model for chromium adsorption.

1.2 Objective

Thus, the main objective of the present study is to undertake experimental and modeling studies on the adsorption of chromium from water. This objective is achieved by initially conducting in batch experiments using an activated carbon and an activated alumina. Based on the adsorption isotherms one of the adsorbents is used for the continuous fixed-bed experiments. Continuous experiments are carried out in a fixed bed column and the parameters varied are flow rate, inlet solution concentration, particle size, and mass of adsorbents. A lumped parameter model was used to predict the adsorption process. Comparison of the predicted and experimental data is finally performed.

CHAPTER 2

LITERATURE REVIEW

2.1 General

Chromium is a naturally occurring element found in rocks, animals, plants, soil and in volcanic dust gases. Chromium is present in the environment in several oxidation states. The most common oxidation states are chromium(0), Chromium(III), and chromium(VI) (ASTDR, 2000). Chromium(VI) and chromium(0) are generally produced by industrial processes (ASTDR, 2000). The most often observed oxidation states of chromium in natural water systems are chromium(III) and chromium(VI) (Kaczynski and Kieber, 1993; Krishnamurthy and Wilkens, 1994).

2.2 Sources of Chromium

Both natural and artificial sources contribute to the occurrence of chromium ion in ground waters. Natural sources of the chromium ion in ground water are due to weathering of chromium bearing minerals. In the earths crust the principal ore of chromium is chromite (FeCr₂O₄) (Weast et al., 1988).

The artificial sources of chromium pollution are mining, leather tanning and cement industries, use in dyes, electroplating, production of steel and other metal alloys, photographic material and corrosive paints (Galvao and Corey, 1987). The artificial sources are the main source of chromium pollution in ground water. Chromium-plating industry effluent is one of the main sources of chromium pollution in aquatic systems. It contains chromium(VI) in the range of 15-300 mg/l (Muthukumaran et al., 1995). The

permissible limit of chromium(VI) for industrial wastewater to be discharged to surface water is 0.1 mg/l (Ranganathan, 2000). Hence it becomes necessary to remove chromium(VI) from wastewaters before discharging them into aquatic systems or on to land.

2.3 Effect of Chromium

Chromium(VI) is present in effluent waters of several different industries. Chromium(VI) is toxic, carcinogenic, mutagenic, and teratogenic (Anderson et al., 1994; Goodgame and Hayman, 1984; Krishnamurthy and Wilkens, 1994; Stollenwerk and Grove, 1985; and Wittbrodt and Palmer, 1995). Chromium affects human physiology, accumulates in the food chain and causes several ailments.

The metallic and trivalent forms of chromium are not normally considered health hazards. Trivalent chromium is an essential trace metal and is required for the proper metabolism of sugar in humans. However, when swallowed, hexavalent chromium chemicals can be poisonous, affecting kidney and liver function. The lethal acute dose for an adult for pure hexavalent chromium compounds is approximately one half teaspoonful. The presence of chromium(III) and chromium(VI) in the environment is the cause of many well documented toxic effects (Galvao and Corey, 1987). The maximum levels permitted in waste water are 5 mg/l for chromium(III) and 0.05 mg/l for chromium(VI). When low levels are present in the environment, Chromium(III) apparently plays an essential role in plant and animal metabolism, while Chromium(VI) is directly toxic to bacteria, plants and animals (Richard and Bourg, 1991). The current

maximum contamination level (MCL) for total chromium in drinking water in the U.S.A. is stipulated by the Environmental Protection Agency (EPA) to be 0.1 mg/l.

Dermal/eye effects vary with the specific form of chromium involved in the exposure. Most hexavalent chromium substances are irritating to eyes, skin and mucous membranes. Unless treated promptly, high exposures can cause permanent injury to the eyes. They also interfere with the healing process of existing cuts and scrapes. Trivalent chromium substances can also be irritating, but this effect is usually related to the acidic nature of some of these compounds (ICDA, 2002). In sensitized individuals all forms can cause allergy related skin rashes. However, even with skin rashes, the hexavalent form is generally a more potent allergen than the trivalent or metallic form. Metallic chromium and chromium alloys are generally inert (ICDA, 2002).

Chromium does not tend to accumulate in the body unless there are ongoing high exposures. Unprotected workers exposed to high levels of dust and mist containing hexavalent chromium may have an increased risk of respiratory cancers. Speculation that exposure to hexavalent chromium can result in a number of other serious long-term illnesses is unsupported. Scientific studies of exposed populations and highly exposed workers have not found a consistent correlation between exposure to hexavalent chromium and any diseases other than respiratory cancers (ICDA, 2002).

2.4 Methods of Chromium(VI) ion Removal from Water

When the concentration of chromium(VI) ion in water sources consistently exceeds the permissible level of 0.1 mg/l it is essential to consider some remedial measures.

Several methods have been proposed to remove chromium(VI) from industrial wastewater. These methods include, such as reduction and precipitation (Philipot et al., 1984), ion exchange (Jorgensen, 1979), electrodialysis, reverse osmosis, solvent extraction (Patterson, 1978), electrochemical precipitation (Kongsricharoern and Polprasert, 1995) and activated carbon adsorption (Huang and Wu. 1975).

2.4.1 Reduction and Precipitation Method

Reduction/precipitation is probably the most commonly used technique for the treatment of industrial effluents containing chromium. Currently the most commonly employed process is reduction of hexavalent chromium to the trivalent form by the addition of a reducing agent (i.e., sodium bisulfite, sulfer dioxide). The chromium sulfate formed is treated with a basic solution, usually lime. As a result of this treatment Cr(OH)₃ precipitates (Lalvani et al., 1998; Ramos et al., 1994). By this method, however, formation of Cr(OH)₃ precipitate causes the formation of waste sludges and secondary saline waste waters (Meinck et al., 1968). The chemical processing of these sludges for recovery of valuable metals is difficult and economical only under certain conditions (Wozniak et al., 1982; Oliver et al., 1976; Scott et al., 1975).

2.4.2 Ion Exchange Method

The principle of ion exchange is widely used to soften or demineralize water and to recover useful by-products from industrial wastes (Liptak, 1974). The hexavalent chromium can be effectively recovered by ion exchange for reuse as a chromate-rich solution. This solution can be recycled into the cooling tower water treatment system, and

the chromate-free water that results from the process may be disposed or further demineralized and reused (Liptak, 1974; Jorgensen, 1979).

2.4.3 Electrodialysis

Electrodialysis is a membrane process driven by electric potential for removing charged species (ions) from an aqueous stream (Letterman, 1999). Electrodialysis is an electrochemical separation process in which ions are transferred through ion exchange membranes by means of a direct current voltage. In a simple electrodylitic cell, negatively charged ions (anions) are drawn toward the positively charged electrode, the anode, and positively charged ions (cations) are drawn towards the negatively charged electrode, the cathode (Patterson, 1978; Letterman, 1999).

2.3.4 Electrochemical precipitation

Removal of chromium from an electroplating wastewater using the electrochemical precipitation (ECP) process has also been studied (Kongsricharoern and Polprasert, 1995). The ECP unit consisted of an electrolytic cell made of two steel plates representing the anode and cathode. The DC power source applied to the ECP unit has a current (I) and electrical potential (E) of 3 to 6 A and 30 to 75 V, respectively. Electroplating wastewater used in the experiments contained Cr⁶⁺ in the range of 215-3860 mg/l, and the pH was 1.5 (Kongsricharoern and Polprasert, 1995).

2.4.5 Adsorption Method

A wide variety of materials have been developed for removal of chromium(VI) ion from waste water on the principal of adsorption. The materials that have been used as adsorbents are activated alumina and activated carbon. Biological based adsorbents have also been used for chromium removal

2.4.5.1 Activated Alumina Adsorption

Removal of chromium(VI) from waste water by using activated alumina is a fixed-bed adsorption method. Use of activated alumina is cheap but its capacity of removal of chromium(VI) from water is less at compare to other adsorbents.

2.4.5.2 Activated Carbon Adsorption

Removal of chromium(VI) from waste water by using activated carbon is a promising method in developed and developing countries. Activated carbons constitute a group of adsorbents with special surface properties such as an extended surface area, a microporous structure, a high adsorption capacity and a high degree of surface reactivity (Corapcioglu and Huang, 1987; and Sontheimer et al., 1988). The surface of activated carbons also exhibit special electrochemical properties and may easily be modified through chemical processing (Dobrowolski et al., 2000). For these reasons, and because of their low cost of production, activated carbons are widely applied as adsorbents, ion-exchange media and catalysts. Activated carbons are widely used to remove toxic ions from water and aqueous solutions (Dobrowolski et al., 2000). The use of activated carbon is important because activated carbon regeneration-reuse can help lower overall treatment

costs and prevent future pollution incidents caused by the disposal of spent carbon laden with hazardous chemicals (Han et al., 2000).

Activated carbon beds have been used for the removal of chromium from industrial waste which is achieved by the accumulation of chromium onto the surface of activated carbon. Results from continuous flow experiments revealed that in excess of 99% chromium removal efficiency can be obtained (Ouki and Neufeld, 1997). By continuous experiment activated carbon does get exhausted and can be regenerated by alkali-acid treatment. The removal of Cr(VI) ions by activated carbon is affected by the pH value of the solution (Miyagawa et al., 1976; Nagasaki, 1974). The maximum capacity of chromium adsorption on activated carbon being exhibited at pH = 6 (Huang and Wu, 1975).

CHAPTER 3

Materials and Methods

3.1 Materials

3.1.1 Activated Carbon and Activated Alumina

Hydrodacro activated carbon and activated alumina, Bhargava Assoc., was used in the present study. The general properties of activated carbon and activated alumina are listed in Tables 3.1 and 3.2, respectively.

Surface area (m ² /g)	487
Iodine number	550
Moisture content (%)	7.9-8.8
Particle density (g/cm³)	1.3 to1.5
Mean pore radius (nm)	2 to 9
Pore volume in the range of 5 to 7500 nm (cm ³ /g)	0.441
Particle size (mm)	0.85 to 1.40
Maximum particle size (mm)	1.40
Minimum particle size (mm)	0.850

Table 3.1 The general properties of activated carbon

Surface area, m ² /g	230
Pore volume, cc/g	0.29 to 0.35
Bulk Density, kg/l	1.10
Actual Density, kg/l	2.05
% Loss on attrition	0.3
Al ₂ O ₃ percentage	93.0
Fe ₂ O ₃ percentage	0.7
Na₂O percentage	0.1
SiO ₂ percentage	6.0
Particle size range, mm	0.3 to 0.6

Table 3.2: The general properties of activated alumina

3.1.2 Chromium (VI) Solution

Various concentrations of chromium(VI) ion solution were used in the batch and continuous experiments of the present study ranging from 20 to 2000 mg Cr^{+6}/l . Specific concentrations of these solutions were obtained by dissolving the required amount of potassium dichromate in known amount of double distilled water. For example, to make a solution of 100 mg Cr^{6+}/l , 0.1 g of $K_2Cr_2O_7$ was added to 1 liter of distilled water.

3.2 Method of Analysis

Chromium(VI) concentration was determined using an UV-Visible spectrometric method. A UV-VIS double beam spectrometer, model: UV-1601, of Shimadzu

Corporation Japan was used for this purpose. The absorbance at 260 nm was used to measure the chromium ion concentration. Initially a calibration plot was generated by observing the absorbance of the 260 nm band for chromium(VI) ion concentrations ranging from 1 to 300 mg/l.

3.3 Experiments

3.3.1 Batch Experiments

Batch experiments were performed for determining the adsorption isotherm of the chromium(VI)-activated carbon and activated alumina-chromium(VI) system. A 50 ml solution of 20, 40, 60, 80, 100, 200, 300, 400, 500, 800, 1000, 1200 and 2000 mg/l chromium(VI) ion concentration were taken in different 250 ml conical flasks. In each conical flask 0.25 g of hydrodacro activated carbon size range was added. The conical flasks were all kept in a shaker, operating at room temperature and at 150 rpm, to ensure proper mixing. The same process was done for activated alumina-chromium(VI) system but the concentration of chromium(VI) ion were 10, 20, 40, 60, 80, 100, 150, 200, 250, 300, 500 and the amount of activated alumina was 0.25 g. The bottles were kept in shakers for 18 h to ensure equilibrium. After 18 h the solution phase chromium concentration was measured as given above and the solid phase chromium concentration was determined by balance.

3.3.2 Continuous Experiments

Continuous fixed bed experiments were performed to generate adsorption data.

Continuous fixed-bed experiments were performed only for the activated carbon-

chromium(VI) system. A schematic diagram of the experimental set up is given in Fig. 3.1. Stock solutions of chromium(VI) ion were allowed to flow through the fixed-bed of activated carbon through a valve, by which the flow rate was controlled. The outlet of the fixed bed was raised slightly above the top of the fixed bed to ensure that adsorption takes place by continuous fixed-bed operation. In these experiments, a glass column of 1.4 cm diameter was used. The parameters varied in the experiments were flow rate, amount of activated carbon, inlet chromium(VI) concentration, and particle size. The following continuous fixed-bed experiments were performed for the fixed bed experiments:

- 1. The flow rate was varied as 5, 10, and 15 ml/min. For these experiments the mass of the activated carbon was kept constant at 15 g, the inlet chromium(VI) concentration was maintained at 100 mg/l, and the particle size of activated carbon was taken as 0.115 cm.
- 2. The mass of activated carbon was decreased to 10 g, and the flow rate and inlet chromium(VI) concentration were maintained at 15 ml/min and 50 mg/l, respectively, and the particle size of activated carbon was taken as 0.115 cm.
- 3. The inlet chromium(VI) concentration was decreased to 50 mg/l, and the flow rate and mass of activated carbon were maintained at 15 ml/min and 15 g, respectively, and the particle size of activated carbon was taken as 0.115 cm.
- 4. The particle size varied as 0.0445, 0.115, and 0.198 cm. For these experiments the other parameters were kept constant. Mass of activated carbon 15 g, inlet chromium(VI) ion concentration 100 mg/l and flow rate 15 ml/min.

5. The mass of regenerated activated carbon was 15 g, and the flow rate and inlet chromium(VI) concentration was maintained at 5 ml/min and 100 mg/l, respectively and the particle size of activated carbon was taken as 0.115 cm.

3.3.3 Regeneration

Regeneration of the above saturated activated carbon was achieved by alkali and acid treatment by using 0.7N NaOH and 5%(v/v) H₂SO₄ solution. Initially, 40 g of the saturated activated carbon was taken in a conical flask and 250 ml of 0.7N NaoH solution was added. The conical flask containing the mixture of NaOH and activated carbon was kept in shaker operating at room temperature and a speed of 150 rpm for 3 h. After 3 h the solution from the conical flask was removed by filtration and again 250 ml of fresh 0.7N NaOH solution was added into the conical flask. This process of adding and removing NaOH solution was repeated 31 times. After the final NaOH treatment the activated carbon was washed with distilled water. Acid treatment was achieved by adding 250 ml of 5%(v/v) H₂SO₄ to the above washed activated carbon. The process, similar to the addition of NaOH solution, was performed 5 times. After the final H₂SO₄ treatment the activated carbon was washed with the distilled water and dried for 24 h at 100°C. The total BET surface area of the fresh and regenerated activated carbon were carried out on a COULTER SA3100 instrument equipped with a version 2.12 SA-view software. The BET surface area of the fresh and regenerated activated carbon was obtained 639 m²/g and 593 m²/g, respectively.

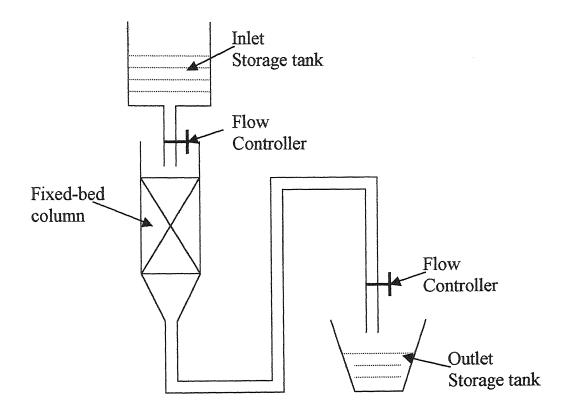


Figure 3.1: Fixed-bed experimental setup for continuous experiments

CHAPTER 4

Modeling

4.1 Modeling Approach

The present study also involved the modeling of fixed bed experimental results. In fixedbed adsorption, the concentrations in the solution phase and the solid phase change with time and with the axial distance from the inlet. In the region where most of the change in concentration occurs is called the mass transfer zone. Initially, when the solution passes through the bed, the solute gets adsorbed in the upper layer of the bed. Consequently, most of the mass transfer occurs in the upper layer of the bed and the effluent concentration at the end of the bed is zero. With time, however, the upper layer gets saturated and the mass transfer zone shifts in the direction of flow. After some time the mass transfer zone reaches near the bottom of the bed, and the concentration of solute at the effluent reaches an appreciable value. The breakthrough point of the bed is said to reached. Subsequently, the effluent concentration increases rapidly until the mass transfer zone passes through the bottom of the bed, and the effluent concentration is nearly equal to the inlet concentration. The curve between effluent concentration and time is called the adsorption curve.

In the present study, the kinetic behavior of the fixed bed column operation is determined by the mechanism or mechanisms controlling the rate at which chromium (solute) is adsorbed onto the surface of activated carbon (adsorbent). The overall rate of adsorption of solute, from a solvent stream flowing through a bed of porous, granular adsorbent represents the following effects:

- (1) Diffusion through the boundary layer of fluid surrounding the adsorbent particle (film or external diffusion)
- (2) Diffusion within the pores of the particle (pore diffusion)
- (3) Diffusion along the surface of the pores (pore-surface diffusion)
- (4) Adsorption on the internal pore surfaces (adsorption)

Some circumstantial evidences indicate that the adsorption process itself is a relatively rapid process and, therefore, is probably not rate controlling. Other three processes are individually or combinations of these processes can be the rate controlling mechanism (Keinath, 1975).

Before describing the modeling approach, it is convenient to describe the following points associated with the adsorption data. Firstly, a fixed bed of certain dimensions has a defined capacity to adsorb the solute entering the bed, that is, the adsorbent would remove the pollutant only until that time when an equilibrium distribution between the liquid and solid phases is reached. Secondly, the adsorption curve of the column depends on mass action equilibrium relationship, the transfer mechanism, and the rate of adsorption (Eagleton, 1953 and Mantell, 1951).

Several methods can be applied to match the experimental results. In the present study lumped parameter model (Keinath, 1975) is used to describe the observed results and is described below. Previous studies involving fluorine adsorption show promising results since a close match between the actual and predicted concentration at the effluent is obtained.

4.2 Material Balance Relationship for Fixed Bed Adsorption Process

The following assumptions are made for the chromium(VI) ion material-balance relationship of the fixed bed adsorption process:

- (1) Axial dispersion in the bed is negligible.
- (2) Concentration gradients in the radial direction are of minor importance, and
- (3) The adsorbents are at fixed positions in the bed.

The material balance relationship for a differential element in the packed bed case is given as:

Input to element = output from element + adsorption + accumulation
$$(4.2.1)$$

For an infinitesimal thickness, dZ, of bed the following mathematical formulations can be made for the solution phase:

Output from element:
$$\left(C + \frac{\partial C}{\partial Z} dZ \right) U$$
 (4.2.3)

Adsorption
$$\rho \left(\frac{\partial q}{\partial t}\right) dZ.dA \qquad (4.2.4)$$

Adsorption
$$\rho \left(\frac{\partial q}{\partial t}\right) dZ.dA \qquad (4.2.4)$$
Accumulation:
$$\varepsilon \left(\frac{\partial C}{\partial t}\right) dZ.dA \qquad (4.2.5)$$

where. U = volumetric flow rate of water, cm³/sec

C = solution-phase chromium(VI) ion concentration, g/cm³

q = solid-phase chromium(VI) ion concentration, g/g

Z = axial distance, cm

t = time, sec

A = cross-sectional area of column, cm²

 ε = void fraction or porosity, dimensionless

Substituting these terms in equation 4.2.1 for a unit cross-section of the bed the partial differential equation is obtained.

$$C.U = \left(C + \frac{\partial C}{\partial Z}dZ\right)U + \rho\left(\frac{\partial q}{\partial t}\right)dZ + \epsilon\left(\frac{\partial C}{\partial t}\right)dZ$$
(4.2.6)

Simplification of equation 4.2.6 gives

$$U\frac{\partial C}{\partial Z} + \varepsilon \frac{\partial C}{\partial t} + \rho \frac{\partial q}{\partial t} = 0$$
 (4.2.7)

The above partial differential equation shows that solution-phase chromium(VI) concentration is a function of both axial distance and time. To facilitate modeling the above partial differential equation is further converted into ordinary differential equation using lumped parameter method (Keinath, 1975).

4.3 Lumped Parameter Model

The lumped parameter method is analogous to using a tank-in-series model to describe non-ideal flow (Fogler, 2000). In the lumped parameter method the fixed bed is divided into 'n' equal volume equilibrium stages, as shown in Figure 4.1.

Use of lumped parameter method requires additional assumptions, which are:

- 1. Segmentation of the packed-bed into a discrete number of elements.
- Both the liquid- and solid-phase concentrations of solute are assumed to be uniform throughout each element.
- 3. Continuity of mass flow of the solute between adjoining elements is be maintained.
- 4. Equilibrium is assumed between solution and solid phase chromium(VI) ion concentration in each stage.

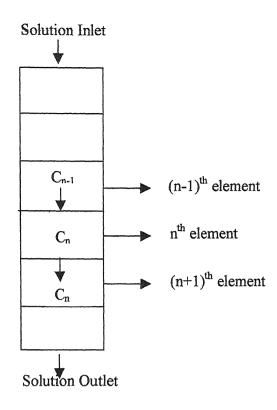


Fig 4.1 Elemental segments in a packed-bed, columnar adsorption contactor

For an adsorption column charged with an adsorbent and then operated in the unsteady-state until the adsorbent is entirely exhausted, the following formulations can be made for an element of the packed-bed which has been designated as element **n** in figure 4.1:

	Solution-phase	Solid-phase
Input to element	$U.C_{n-1}$	0
Output from element	$U.C_n$	0
Adsorption	$\rho.R_{_{An}}.V$	$\rho.R_{_{An}}.V$
Accumulation	$\varepsilon \left(\frac{dC_n}{dt}\right)V$	$\rho\!\!\left(\!\frac{dq_{_{\boldsymbol{n}}}}{dt}\!\right)\!\!V$

where, $C_n = \text{chromium(VI)}$ ion concentration in the n^{th} element

 C_{n+1} = chromium(VI) ion concentration of the stream to the $(n+1)^{th}$ element

V = volume of each element in, cm³

 R_{An} = rate of adsorption for the nth element in, g/g of solid/second

n = no. of elements in the packed-bed

Hence, the solution phase chromium (VI) ion material balance results in

$$U.C_{n-1} = U.C_n + \rho.R_{An}.V + \varepsilon \left(\frac{dC_n}{dt}\right)V$$
(4.3.1)

Rearranging equation 4.3.1 yields

$$\frac{dC_n}{dt} = \left(\frac{U}{\varepsilon V}\right) (C_{n-1} - C_n) - \left(\frac{\rho}{\varepsilon}\right) R_{An}$$
(4.3.2)

Similarly, chromium(VI) ion material balance relationship for solid-phase is

$$0 = 0 - \rho R_{An} \cdot V + \rho \left(\frac{dq_n}{dt}\right) V \tag{4.3.3}$$

Equation 4.3.3 simplifies to

$$\frac{\mathrm{dq_n}}{\mathrm{dt}} = R_{\mathrm{An}} \tag{4.3.4}$$

The rate of adsorption (R_{An}) depends on the rate-controlling step in fixed bed adsorption.

If pore diffusion controls the overall process, then

$$R_{An} = \frac{dq_{n}}{dt} = K_{p}.A_{p}.(C_{n} - C_{n}^{*})$$
(4.3.5)

where, $K_P = \text{mass transfer coefficient (pore), cm/sec}$

 A_p = external interfacial transfer area for adsorbent, cm²/cm³

 C^* = solution-phase concentration of solute considered to be in equilibrium

with the outer surface on the adsorbent particles, g/cm³

K_P*A_P can be determined from the following correlation (Keinath, 1975)

$$K_{P}.A_{P} = \frac{60 * D_{pore}}{D_{P}^{2}} (1 - \varepsilon_{p})$$
 (4.3.6)

For liquids, the pore diffusivity (D_{pore}) may be approximated by the relationship (Keinath, 1975)

$$D_{pore} = D_1.X/2$$
 (4.3.7)

Where, $D_{pore} = pore diffusivity, cm^2/sec$

X = internal porosity of adsorbent particles, dimensionless

 $D_1 = diffusivity of solute in solvent, cm^2/sec$

If film or external diffusion controls the overall process, then

$$R_{An} = \frac{dq_{n}}{dt} = K_{f} \cdot A_{p} \cdot (C_{n} - C_{n}^{*})$$
 (4.3.8)

where, $K_f = \text{film-diffusion controlled mass transfer coefficient, cm/sec}$

For the external diffusional process the mass transfer coefficient is determined by correlation involving the mass transfer factor, j_d.

$$j_d = 5.7.(N_{Re})^{-0.78}$$
 for $30 > N_{Re} > 1$ (4.3.9)

where,
$$j_d = \left(\frac{K_f A}{U}\right) \left(\frac{\upsilon}{D_1}\right)^{2/3}$$
 (4.3.10)

$$N_{Re} = \text{Reynold number} = \left(\frac{UD_p}{Av(1-\epsilon)}\right)$$
 (4.3.11)

 $v = \text{kinematic viscosity of water, cm}^2/\text{sec}$

The rate of adsorption (R_{An}) depends on the rate-controlling step in fixed bed adsorption. The rate controlling step is either external film diffusion or intra-particle diffusion or both.

Hence, the general equation for the rate of adsorption is given by

$$R_{An} = \frac{dq_n}{dt} = K.A_s.(C_n - C_n^*)$$
 (4.3.12)

where, K.A_s = mass transfer coefficient based on external surface area

= K_P . A_P , if pore diffusion controls the overall process, or

=K_f.A_s, if external diffusion controls the overall process, or

$$= \frac{1}{\left(\frac{1}{K_{P}.A_{P}} + \frac{1}{K_{f}.A_{s}}\right)}$$
 for both external and internal diffusions controlled.

Additionally, the adsorption isotherm for the chromium(VI) ion and activated carbon is given by

$$q_n = \left(\frac{a}{1 + bC^*}\right)C^* \tag{4.3.13}$$

where a,b = langmuir constants

Equation 4.3.2 and 4.3.13 can be solved by finite difference method resulting in the following two equations for solution and solid phase concentration with respect to time. Solution-phase concentration equation is given by

$$C_{n}|_{t+\Delta t} = C_{n}|_{t} + e.\Delta t \left(C_{n-1}|_{t} - C_{n}|_{t}\right) - f.\Delta t \left(C_{n}|_{t} - \frac{q_{n}|_{t}}{(a-b.q_{n}|_{t})}\right)$$
(4.3.14)

Solid-phase concentration equation is given by

$$q_{n}|_{t+\Delta t} = q_{n}|_{t} + K.A_{s}.\Delta t \left(C_{n}|_{t} - q_{n}|_{t}/(a-b.q_{n}|_{t})\right)$$
 (4.3.15)

where, e and f are constants given by

$$e = \left(\frac{U}{\varepsilon V}\right)$$
 and $f = \left(\frac{\rho}{\varepsilon}\right) K.A_s$

To model the adsorption of chromium(VI) ion on activated carbon a C-program was developed. The two assumptions are made in that program:

- 1. Linear isotherm was assumed for a considerable region.
- 2. In place of actual inlet chromium(VI) ion concentration, apparent chromium(VI) ion concentration was used.

The algorithm for this program is given in Fig 4.2 and code is given in Appendix C.

The standard deviation, σ , was calculated for comparing the model and experimental results is and given as:

$$\sigma = \sqrt{\sum \frac{(C_{\text{experiment al}} - C_{\text{model}})^2}{N}}$$
 (4.3.16)

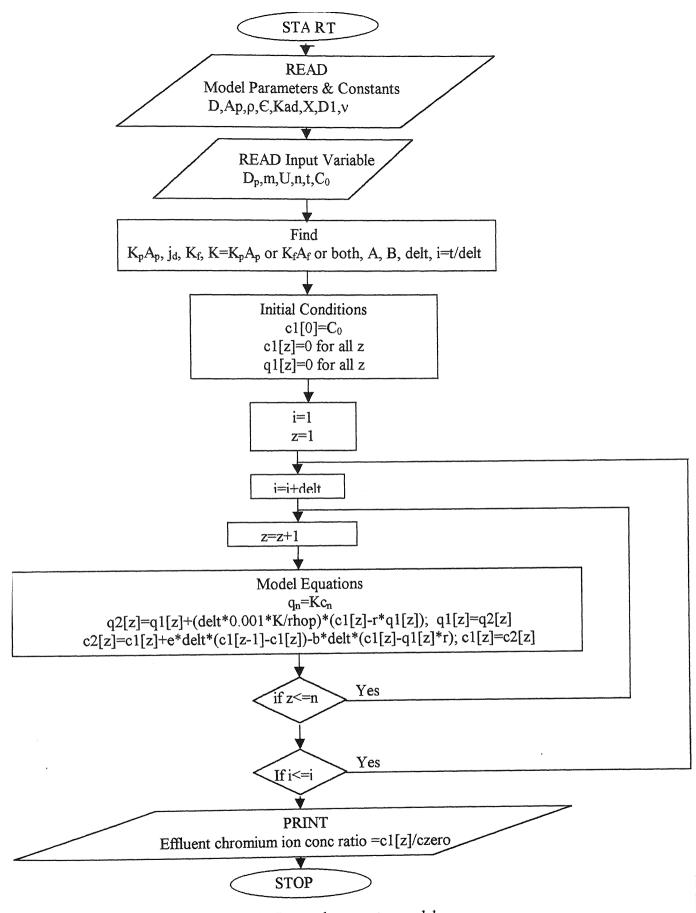


Figure 4.2: Flow chart for the Lumped parameter model

CHAPTER 5

RESULTS

In this chapter experimental and model results for the adsorption of chromium(VI) ion are presented. Two types of experiments were considered: Batch and Continuous.

5.1 Batch Studies

Batch experiments were carried out to provide the equilibrium isotherm of chromium(VI) ion adsorption. The isotherms were achieved by plotting the solution phase chromium(VI) ion concentration (mg/l) versus solid phase chromium ion concentration (mg/g) obtained at equilibrium (18 h). Batch experiments results are given in Figs 5.1 and 5.2 and tabulated as Tables A1 and A2 in appendix A, for the activated carbon-chromium(VI) and the activated alumina-chromium(VI) systems, respectively. Fig. 5.1 reveals that the adsorption isotherm can be best represented by a Langmuir isotherm (shown as a solid line) expressed as $q = a.C^*/(1+b.C^*)$, where, q is the equilibrium solid phase concentration, C* is equilibrium solution phase concentration, and a and b are the Langmuir constants. The choice of Langmuir isotherm was based on the smallest standard deviation observed. The Langmuir constants, a and b, have values of 0.178 and 0.01, respectively. In Fig. 5.2 the isotherm for the activated aluminachromium(VI) system is plotted. This figure shows that the adsorption isotherm can also be best represented by a Langmuir isotherm as given above with Langmuir constants, a and b, having values of 0.028 and 0.003, respectively. Previous studies suggest that for the chromium(VI)-activated carbon system, the adsorption isotherm is either best

represented by a Langmuir isotherm (Huang et al., 1977; Lalvani et al., 1998; Aggarwal et al., 1999) or by a Freundlich isotherm (Han et al., 2000; Ramos et al., 1994).

5.2 Continuous Studies

The adsorption isotherms shown in Figs 5.1 and 5.2 reveal that for the same conditions the amount of chromium(VI) ions adsorbed on activated carbon was higher than that on activated alumina. Therefore, continuous fixed-bed experiments were performed using activated carbon as the adsorbent since this activated carbon appears to provide a larger adsorption capacity for chromium.

For the fixed-bed experiments, the dimensionless effluent chromium(VI) ion concentration, C/C₀, is plotted versus elapsed time, the adsorption curve, for various values of flow rate, mass of adsorbent, inlet concentration, and adsorbent particle size. The effect of these experimental conditions on the adsorption curve are shown in Figs. 5.3 to 5.6.

In Fig. 5.3, the fixed-bed results are plotted for different flow rates. The mass of activated carbon, inlet chromium(VI) ion concentration, and particle size were constant at 15 g, 100 mg/l, and 0.115 cm, respectively. The different flow rates considered are 5, 10, and 15 ml/min. The tabular results of these three continuous experiments are also given in Tables A3, A4, and A5, in Appendix A. Examination of Fig 5.3 reveals that the break through point occurs much quicker at higher flow rates than at lower flow rates. After break through occurs, the effluent chromium(VI) ion concentration, C/C₀ increases rapidly with time till the C/C₀ reaches a value of 0.6 to 0.7.

Subsequently, the C/C_0 value increases gradually. Interestingly, however, the effluent chromium(VI) ion concentration does not reach the inlet C_0 value even after 24 h.

In Fig. 5.4 the effect of mass of activated carbon on the adsorption curve is presented. The mass of activated carbon considered were 10 and 15 g. The flow rate, inlet chromium(VI) ion concentration, and particle size were kept constant at 15 ml/min, 50 mg/l, and 0.115 cm, respectively. Tabular results of these two experiments are given in Table A6 and A7, respectively in Appendix A. From Fig. 5.4 it is observed that for lower mass of activated carbon the break through point is achieved sooner. Thereafter, C/C_0 rises rapidly till a value of ~ 0.7 for 10 g and ~ 0.6 for 15 g. As before, the C/C_0 increases gradually after this initial rapid increase.

The effect of inlet chromium(VI) ion concentration, C_0 , on the adsorption curve is shown in Fig. 5.5. Two inlet chromium(VI) ion concentrations used are 50 and 100 mg/l. The flow rate, mass of activated carbon, and particle size were kept constant at 15 mg/l, 15 g, and 0.115 cm, respectively. Tabular results of these two fixed-bed experiments are given in Appendix A as Tables A3 and A6, respectively. Examination of Fig 5.5 reveals that for higher C_0 values the break through point is achieved sooner. As before the C/C_0 value initially increases rapidly till a value of ~ 0.6 for $C_0 = 50$ mg/l and a value of ~ 0.7 for $C_0 = 100$ mg/l. The C/C_0 values then increases gradually with time.

The effect of particle size on the adsorption curve is shown in Fig. 5.6. The particle sizes considered are 0.0445, 0.115, and 0.198 cm. The adsorption curve is shown upto 4 h to clearly bring out the effect of particle size. The mass of activated carbon, flow rate, and inlet chromium(VI) ion concentration were taken as 15 g, 15 ml/min, and 100 mg/l, respectively. Tabular results of these three continuous experiments are given in

Tables A3, A9 and A10, respectively in Appendix A. Fig. 5.6 shows that for larger particle size the break through point is achieved sooner. After the break through point the C/C_0 value initially increases rapidly and then gradually, similar to the previous cases.

Fig. 5.7 shows the break through curve of activated carbon after regeneration. The mass of regenerated activated carbon, flow rate, inlet chromium(VI) ion concentration, and particle size were taken as 15 g, 5 ml/min, 100 mg/l, and 0.115 cm, respectively. The adsorption curve on fresh activated carbon performed with the same parameters are also shown for reference. Tabular results of these two continuous experiments are presented in Appendix A as Tables A5 and A8 respectively. Fig. 5.7 shows that after regeneration, the adsorption capacity of activated carbon is reduced. This is evident from the earlier break through point and displacement of the curve to lower times.

5.3 Modeling Studies

From the adsorption curves shown in Figs. 5.3 to 5.6 it is observed that there are essentially three regions present. The first region is where there is no outlet chromium(VI) concentration; the second region is where the outlet chromium(VI) concentration reaches a significant value and then increases rapidly, and the final region is when the outlet chromium(VI) concentration increases gradually but does not reach the outlet concentration even after 25 h. For example, in Fig. 5.3 and for a flow rate of 5ml/min, the first region is upto ~ 4 h, the second region is from ~ 4 h to ~ 8 h, and the third region is beyond 8 h.

Modeling of the adsorption curves was tried by determining the outlet concentration at different times based on the various input variables known a priori. The

only unknown parameter involved is the chromium(VI) ion diffusivity, which was adjusted to give the best fit curve. Results from the modeling study based on the best value of diffusivity was not able to represent the three regions in the adsorption curve discussed above. The main drawback occurred in representing the third region of the adsorption curve since the gradual increase of C/C₀ with time was not achieved. To simplify modeling of the fixed-bed experiments, thus, only the first two regions were considered, i.e., the break through point and the rapid increase of C/C₀ values. Furthermore, to facilitate modeling the C₀ value was taken as the effluent chromium(VI) concentration at the time where the third region of gradual C/Co increase begun. This apparent C₀ value was defined as C₀^a, which was about 0.6 to 0.75 of the actual C₀ value. The modeling results based on this C_0^a value and the required input variables are shown in Figs. 5.8 to 5.14 along with the corresponding experimental data. Furthermore, only external transport was considered, i.e., external film diffusion controls the mass transfer process. The only adjustable parameter was the chromium ion diffusivity, which was obtained by fitting the model to the experimental data. The best value (by inspection), of the chromium ion diffusivity was constant, 4.31*10⁻⁵ cm²/sec, for all the model curves shown in Figs. 5.8 to 5.14. The value of diffusivity is well within the range of liquid diffusivities in water (Treybol, 1981).

Based on the constant value of diffusivity a good representation of the experimental adsorption curve was obtained as shown in Figs. 5.8 to 5.14, except for 2 cases. Further comparison between the model and experimental results were performed by determining the standard deviations. The standard deviation values for the seven experiments are shown in Table 5.1. Examination of Table 5.1 reveals that the standard

deviation between the experimental and model results, given in the sixth column, are satisfactory except for two cases, experiment number 3 and 6. The unsatisfactory fit is also clearly observed in Figs. 5.10 and 5.13. In these two experiments either the flow rate was low or the particle size was small. Under both of these conditions it appears that the internal transport becomes important. The effect of internal transport was not considered in the present study. Thus the model is able to represent the experimental data reasonably well in the first two regions based on the apparent C₀ value.

In summary, adsorption curves for the activated carbon-chromium(VI) system were obtained for different sets of experimental conditions in which three regions were observed. Modeling of the adsorption curves was achieved for the first two regions based on an apparent inlet chromium(VI) ion concentration and a constant chromium ion diffusivity. Comparison of the experimental modeling results reveals that the two regions of the adsorption curve can be reasonably represented.

Exp. No.	Experimental conditions			Standard deviation for the External	
	Mass	Inlet Cr(VI) ion	Flow rate	Particle	Transport model
	(g)	concnetration (mg/l)	(ml/min)	diameter (cm)	
1	15	100	15	0.115	0.030
2	15	100	10	0.115	0.058
3	15	100	5	0.115	0.141
4	15	50	15	0.115	0.045
5	10	50	15	0.115	0.045
6	15	100	15	0.044	0.136
Calandra Dave, Against printing has been defined at the Manufact AME of Children 46 to	15	100	15	0.198	0.034

Table 5.1: Standard deviation calculation for external transport model

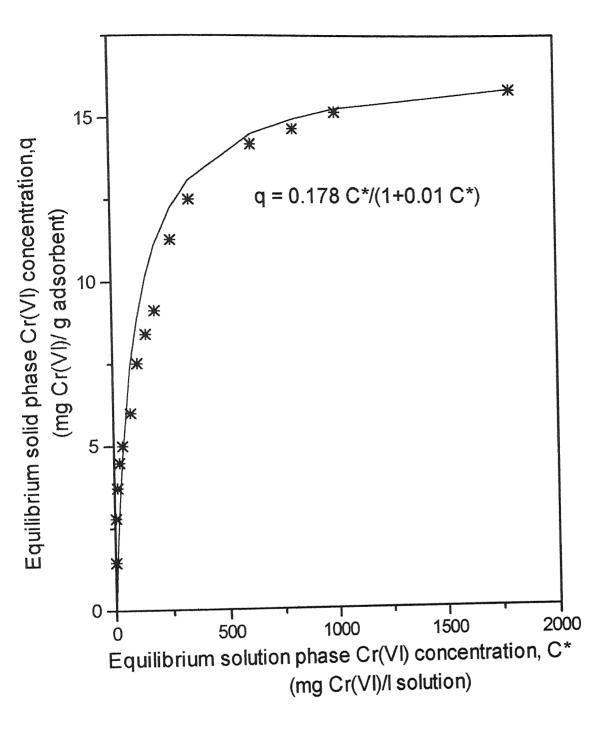


Fig. 5.1: Adsorption isotherm for chromium(VI) and activated carbon system

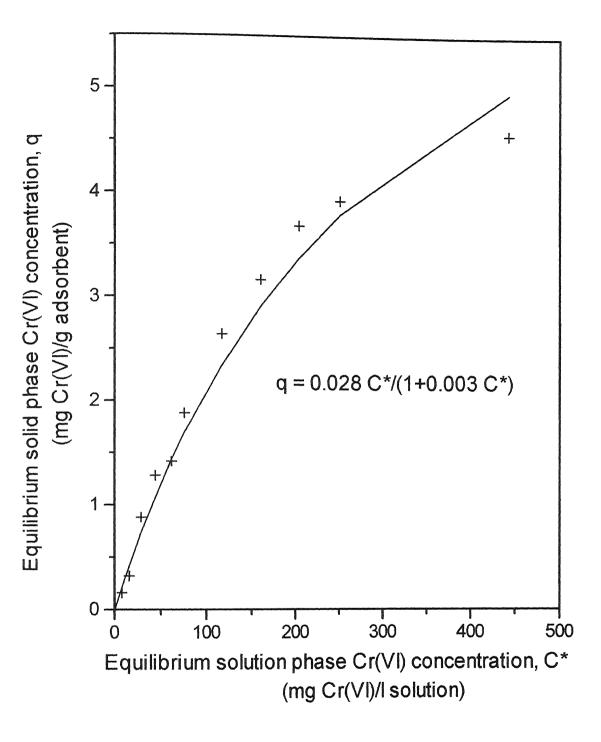


Fig. 5.2: Adsorption isotherm for chromium(VI) and activated alumina system

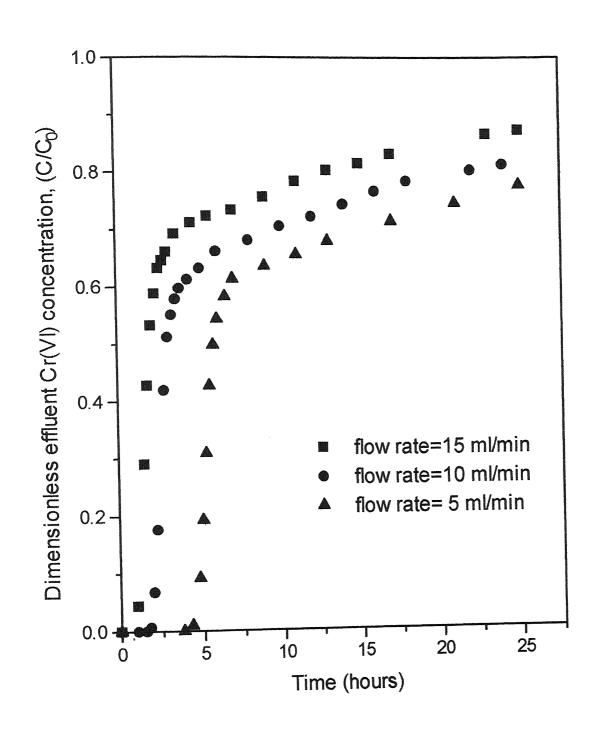


Fig. 5.3: Effect of flow rate on dimensionless chromium(VI) ion concentration.

Mass of activated carbon = 15 g, inlet chromium(VI) ion concentration = 100 mg/l and particle size = 0.115 cm.

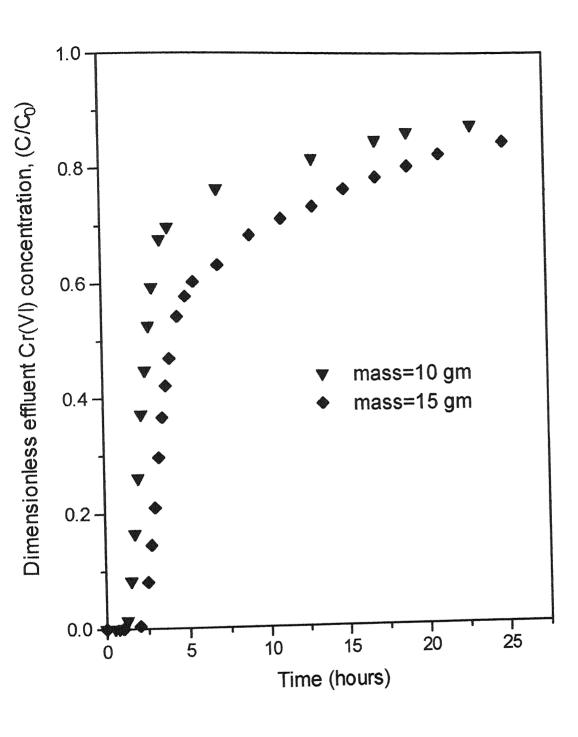


Fig. 5.4: Effect of mass of activated carbon on dimensionless effluent Cr(VI) concentration. Inlet chromium(VI) ion concentration = 50 mg/l, flow rate = 15 ml/min, and particle size = 0.115 cm

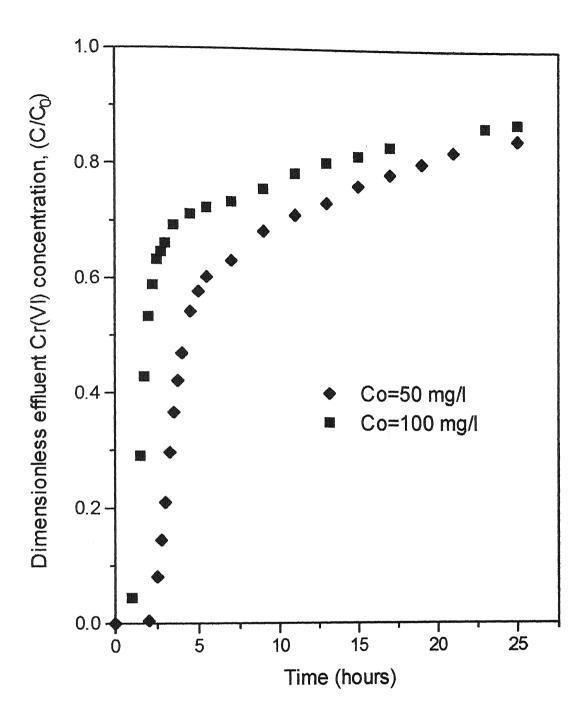


Fig. 5.5: Effect of chromium(VI) ion concentration on dimensionless effluent chromium(VI) ion concentration. Mass of activated carbon = 15 g, flow rate = 15 ml/min, and particle size = 0.115 cm

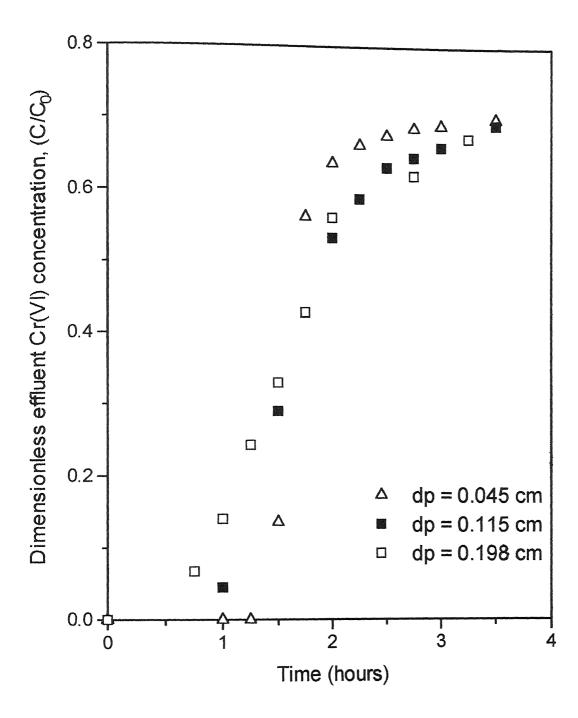


Fig. 5.6: Effect of particle size on dimensionless effluent chromium(VI) ion concentration. Inlet chromium(VI) ion concentration = 100 mg/l, flow rate = 15 ml/min, and mass of activated carbon = 15 g

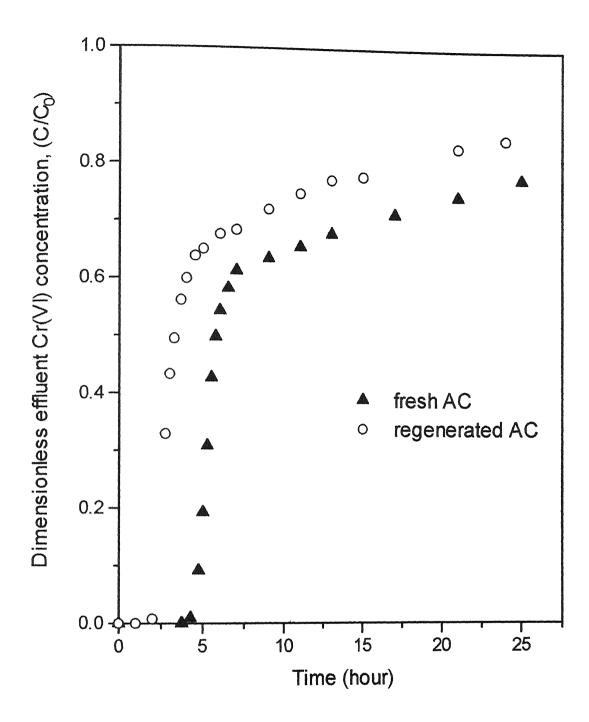


Fig. 5.7: Effect of regeneration of activated carbon (AC) on dimensionless effluent chromium(VI) ion concentration. Inlet chromium(VI) ion concentration = 100 mg/l, flow rate = 5 ml/min, mass of activated carbon = 15 g, and particle size = 0.115 cm

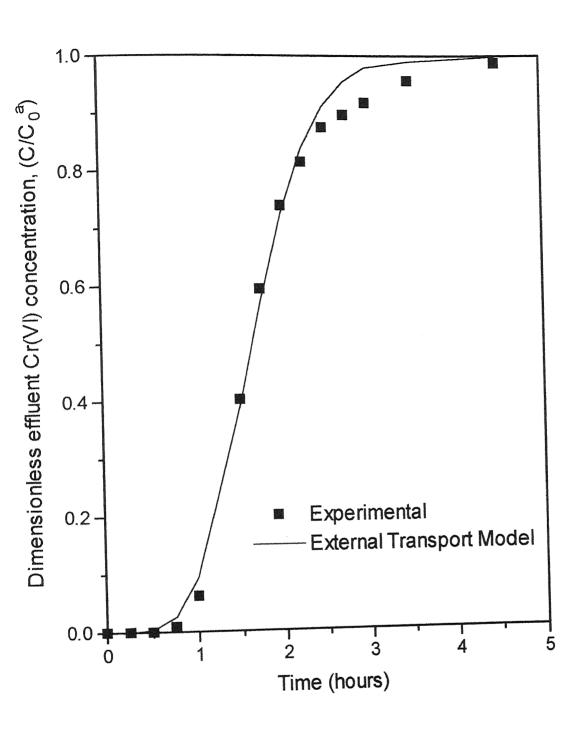


Fig. 5.8: Comparison of external transport model with experimental results. Mass Of activated carbon = 15 g, inlet chromium(VI) ion concentration = 100 mg/l, flow rate = 15 ml/min, particle size = 0.115 cm, and apparent inlet chromium(VI) ion concentration $(C_0^a) = 72$ mg/l

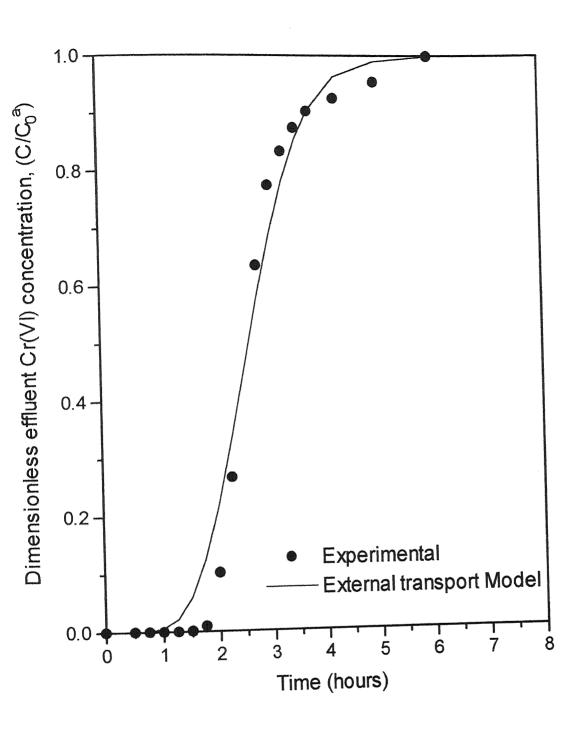


Fig. 5.9: Comparison of external transport model with experimental results. Mass of activated carbon = 15 g, inlet chromium(VI) ion concentration = 100 mg/l, flow rate = 10 ml/min, particle size = 0.115 cm, and apparent inlet chromium(VI) ion concentration $(C_0^a) = 68$ mg/l

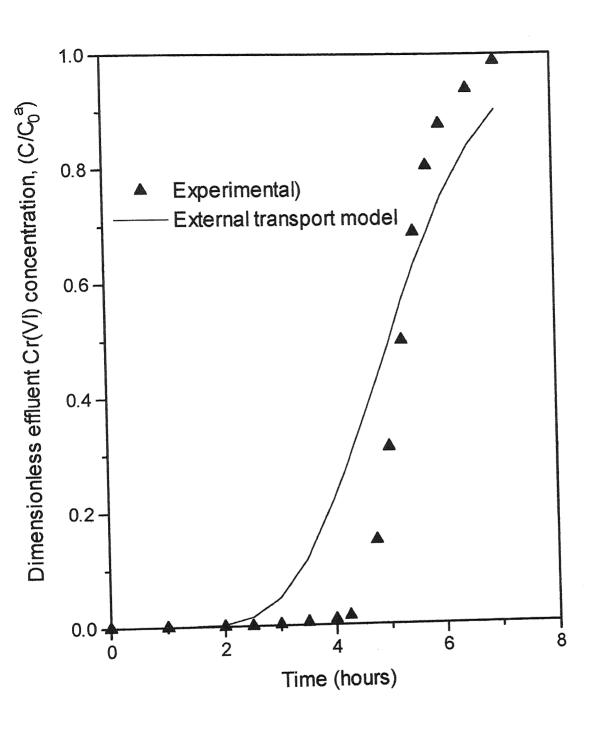


Fig. 5.10: Comparison of external transport model with experimental results. Mass of activated carbon = 15 g, inlet chromium(VI) ion concentration = 100 mg/l, flow rate = 5 ml/min, particle size = 0.115 cm, and apparent inlet chromium(VI) ion concentration $(C_0^a) = 62$ mg/l

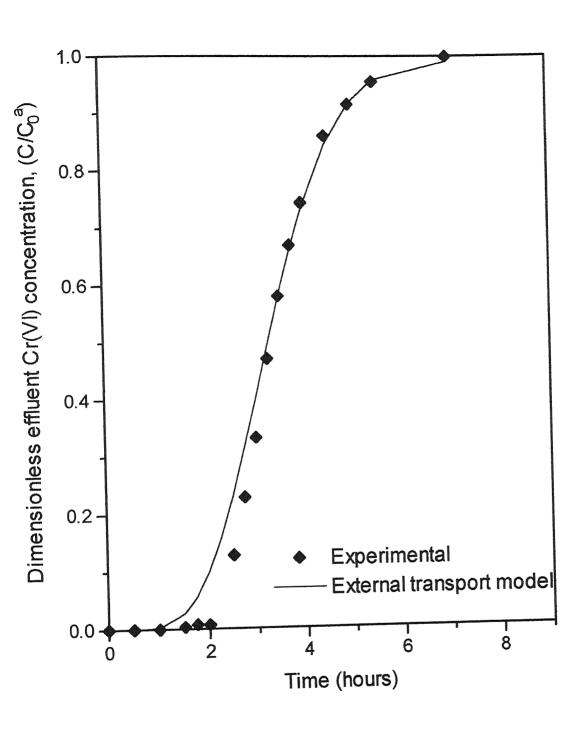


Fig. 5.11: Comparison of external transport model with experimental results. Mass of activated carbon = 15 g, inlet chromium(VI) ion concentration = 50 mg/l, flow rate = 15 ml/min, particle size = 0.115 cm, and apparent inlet chromium(VI) ion concentration $(C_0^a) = 32$ mg/l

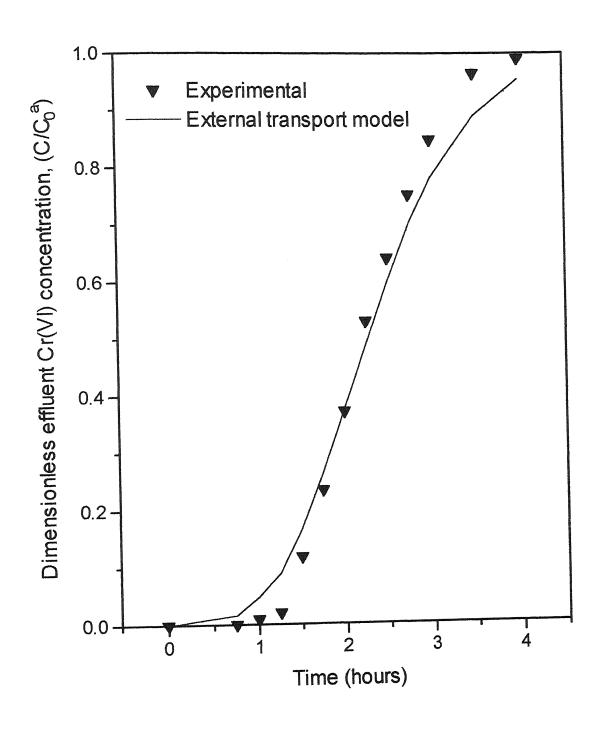


Fig. 5.12: Comparison of external transport model with experimental results. Mass of activated carbon = 10 g, inlet chromium(VI) ion concentration = 50 mg/l, flow rate = 15 ml/min, particle size = 0.115 cm, and apparent inlet chromium(VI) ion concentration $(C_0^a) = 35$ mg/l

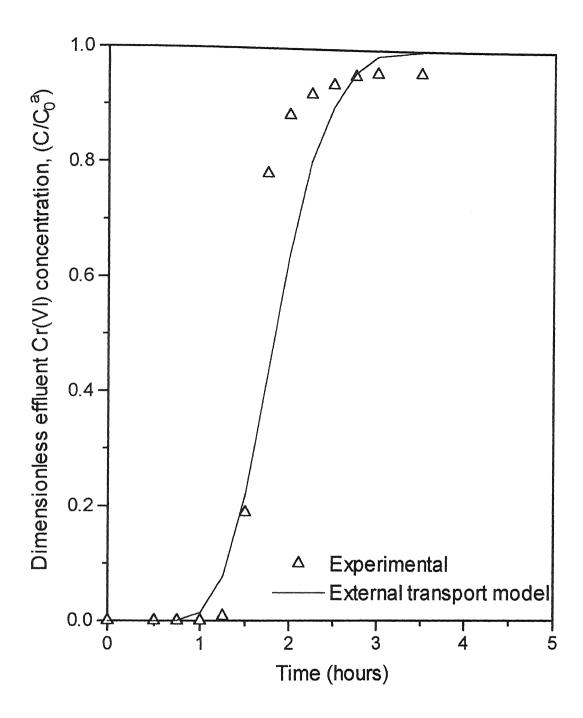


Fig. 5.13: Comparison of external transport model with experimental results. Mass of activated carbon = 15 g, inlet chromium(VI) ion concentration = 100 mg/l, flow rate = 15 ml/min, particle size = 0.045 cm, and apparent inlet chromium(VI) ion concentration $(C_0^a) = 72$ mg/l

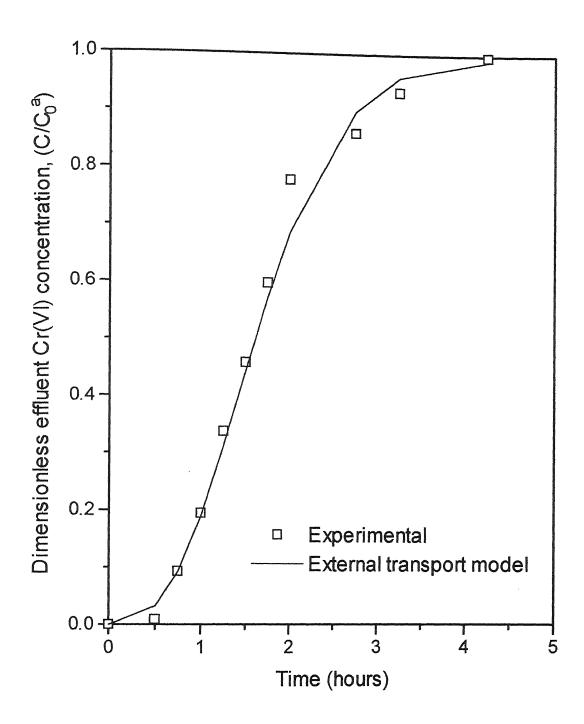


Fig. 5.14: Comparison of external transport model with experimental results. Mass of activated carbon = 15 g, inlet chromium(VI) ion concentration = 100 mg/l, flow rate = 15 ml/min, particle size = 0.198 cm, apparent inlet chromium(VI) ion concentration $(C_0^a) = 72$ mg/l

CHAPTER 6

6.1 Conclusions

Based on the results of the present study the following conclusions can be made:

- Activated carbon and activated alumina are able to adsorb chromium(VI) ion.
- The adsorption isotherms for chromium(VI)-activated carbon and chromium(VI)-activated alumina system are best represented by Langmuir isotherm. The Langmuir constants, a and b, had values of 0.178 and 0.01 for chromium(VI)-activated carbon, and 0.028 and 0.003 for chromium(VI)-activated alumina.
- The amount of chromium(VI) ion adsorbed on activated carbon is higher than activated alumina.
- The continuous fixed-bed experiments reveal that the change in effluent chromium(VI) ion concentration with time depends on flow rate, mass of activated carbon, inlet chromium(VI) ion concentration, and particle size.
- The adsorption curves obtained by continuous experiments essentially had three distinct region.
- Regenerated activated carbon capacity is lower than the fresh activated carbon.
- Modeling results involving external transport as the rate limiting step for mass transfer predicts the adsorption of chromium(VI) by activated carbon reasonably well for the first two regions based on an apparent inlet chromium(VI) concentration, which is 0.6 to 0.75 of the actual C₀ value. Furthermore, the only adjustable parameter, the chromium(VI) ion diffusivity, had a value of 4.31*10⁻⁵ cm²/sec.

• With an increase in flow rate the external transport model predicts the experimental results better than at lower flow rate and for smaller particle size.

6.2 Suggestions for Future Studies

Based on the observations of the present study, further studies can be carried out along the following:

- In the present model the varied parameters are influent flow rate, mass of activated carbon (adsorbent), inlet chromium(VI) concentration, and particle size.

 A model can be developed using one more variable such as diameter of column and pH of the inlet solution.
- In the present model axial dispersion is neglected but at very low flow rates axial dispersion may be significant.
- Presence of other ions and dissolved solids in water also affect the adsorption of chromium(VI) ion. This effect can also be studied.
- The Lumped parameter model can be improved to better represent the adsorption curve.

References

- Agency for Toxic Substances and Disease Registry (ATSDR), Toxicological profile for chromium. *U.S. Department of Health and Human Services*. Public Health Service (1993).
- Agency for Toxic Substances and Disease Registry (ATSDR), Toxicological profile for chromium (Update). *U.S. Department of Health and Human Services*. Public Health Service (1998).
- Agency for Toxic Substances and Disease Registry (ATSDR), Toxicological profile for chromium (Update). U.S. Department of Health and Human Services.
 Public Health Service (2000).
- Aggarwal, D., Goyal, M., Bansal, R. C., Adsorption of chromium by activated carbon from aqueous solution. *Carbon*, 37(1999)1989.
- Anderson, L. D., Kent, D. B., Pavis, J. A., Batch Experiments Characterizing the Reduction of Cr(VI) Using Suboxic Material from a Mildly Reducing Sand and Gravel Aquifer. *Environ. Sci. Technol.*, 28(1994)178.
- Corapcioglu, M. O., Huang, C. P., The adsorption of heavy metals onto hydrous activated carbon. *Carbons*, 25(1987)569.
- Dobrowolski, R., Stefaniak, E., Study of Chromium(VI) Adsorption from Aqueous Solution on to Activated Carbon. Adsorption Science & Technology, 18(2000)97.
- Eagleton, L. C., Biss, H., Drying of Air in Fixed Beds. Chemical Engineering Progress, 49(1953)543.
- Fogler, H. S., Elements of Chemical Reaction Engineering, 2nd edition, (2000)
- Galvao, L. A. C., Corey, G., Serie Vigilancia. 5 Cromo. Centro Panamericano de Ecologia Humana y Salud, Organizacion Mundial de la Salud (1987).
- Gupta, S., Dey, G. C., Agarwal, A. B. L., Deo, G., Defluoridation of Water Using Activated Alumina: Experimental and Modeling Studies. Submitted to Water Research, (2002)

- Goodgame, D. M. L., Hayman, P. B., Formation of Water-Soluble Chromium(V) by the Interaction of Humic Substances and Low Molecular Weight Ligands. Inorg. Chim. Acta, 91(1984)113.
- Han, I., Mark, A. S., Batchelor, B., Removal of Hexavalent Chromium from Groundwater by Granular Activated Carbon. Water Environmental Research, 72(2000)29.
- Huang, C. P., Wu, M. H., Chromium removal by carbon adsorption. J. Wat. Pollut. Control, 47(1975)2437.
- Huang, C. P., Wu, M. H., The removal of Chromium(VI) from dilute aqueous solution by activated carbon. Water Research, 11(1977)673.
- IARC, IARC Monographs on the Evaluation of the Carcinogenic Risk of Chemicals to Humans; Chromium, Nickel, and Welding, International Agency for Research on Cancer, World Health Organization, Lyon, France, Vol. 49(1990).
- International Chromium Development Association, news, june, 2002.
- Jorgensen, S. E., Industrial Wastewater Management. Elsevier, New York, (1979)81.
- Kaczynski, S. E., Kieber, R. J., Aqueous Trivalent Chromium Photoproduction in Natural Waters. *Environ. Sci. Technol.*, 27(1993)1572.
- Keinath, T. M., Mathematical Modeling for Water Pollution Control Process,
 Chapter Modeling and Simulation of the performance of Adsorption Contactors.
 Ann Arbor Science Publishers, Inc., Ann Arbor, Michigan, (1975)1.
- Kongsricharoern, N., Polprasert, C., Electrochemical precipitation of chromium from an electroplating wastewater. Water Sci. Technol., 31(1995)109.
- Krishnamurthy, S., Wilkens, M. M., Environmental Chemistry of Chromium.
 Northeast. Geol., 16(1994)14.
- Lalvani, S. B., Wiltowski, T., Hubner, A., Weston, A., Mandich, N., Removal of Hexavalent Chromium and Metal Cations by a Selective and Novel Carbon Adsorbent. *Carbon*, 36(1998)1219.
- Letterman, R. D., Water quality and Treatment, fifth edition, A handbook of community water supplies, American water works association (1999).
 पुरुषोत्तम काशीनाथ केनकर पुस्तकालक

- Liptak, B. G., Environmental Engineer's hand book, vol 1, Water Pollution: Chilton Book Company, Radnor, Pennsylvania, (1974).
- Low, K.S., Lee, C. K., Ng, A. Y., Journal of Environ Sci Health, A, 32(1997)1849.
- Mukherjee, A. G., (Ed) Environmental Pollution and Health Hazards: Causes and Control (Galgotia, N.D.), (1986).
- Mantell, C. L., Adsorption. McGraw Hill, Inc., New York, 2nd edition, (1951).
- Meinck, F. et al., Industric-Abwasser.Gustaw fischer, Stuttgart, 4th ed. (1968).
- Metcalf and Eddy, Wastewater Engineering, Treatment Disposal Reuse, Third
 Edition, (1995)
- Miyagawa, T., Ikeda, S., Koyama, K., Jpn. Kokai, 76(1976)417.
- Mukherjee, A. G., (Ed) Environmental Pollution and Health Hazards: Causes and Control (Galgotia, N.D.), (1986).
- Muthukumran, K., Balasubramanian, N., Ramakrushna, T. V., Removal and recovery of chromium from plating waste using chemically activated carbon. *Metal finishing*, Nov (1995).
- Nagasaki, Y., Removal of metal ions from waste water with coal adsorbent.
 Japan Kokai, 74(1974)477.
- Oliver, B. G., Carey, J. M., Water Res., 10(1976)1077.
- Ouki, S. K., Neufeld, R. D., Use of activated carbon for the recovery of chromium from industrial wastewaters. *Journal of Chemical Technology and Biotechnology*, 70(1997)3.
- Patterson, J. W., Water Treatment Technology, third ed., Ann Arbor Science, Ann Arbor Michigan, MI (1978).
- Peavy, H. S., Rowe D. R., George T., Environmental Engineering, International Edition, (1988).
- Philipot, J. M., Chaffange, F., Sibony, J., Hexavalent chromium removal from drinking water. Water Sci. Technol. 17(1984)1121.
- Powell, R. M., Puls, R.W., Hightower, S. K., Sabatini, D. A., Coupled Iron Corrosion and Chromate Reduction: Mechanisms for subsurface Remediation. Environ. Sci. Technol., 29(1995)1913.

- Ramos, R. L., Martinez, A. J., Coronado, R. M. G., Adsorption of Chromium(VI) from Aqueous Solutions on Activated Carbon. *Wat. Sci. Tech.*, 30(1994)191.
- Ranganathan, K., Chromium removal by activated carbons prepared from Casurina equisetifolia leaves. *Bioresource Technology*, 73(2000)99.
- Richard, F. C., Bourg, A. C. M., Aqueous Geochemistry of Chromium: A Review. Wat. Res. 25(1991)807.
- Scott, D. S., Horlings, H., Environ. Sci. Technol., 9(1975)849.
- Sharma, Y. C., Adsorption of Cr(VI) onto Wollastonite: Effect of pH. Indian Journal of Chemical Technology, 8(2001)186.
- Siegel, D. M., Carcinogenicity of chromium via ingestion. Memo to Standards/Criteria Wrokgroup members, dated August 7, (1990).
- Sontheimer, H., Crittenden, J. C., Summers, R. S., Activated carbon for water treatment. Am. Water works Assoc. Res. Found., Denver, Colo (1988).
- Stollenwerk, K. G., Grove, D. B., Adsorption and Desorption of Hexavalent Chromium in an Alluvial Aquifer Near Telluride, Colorado. J. Environ. Qual., 14(1985)396.
- Treybal, R. E., Mass-Transfer Operations, 3rd edition, (1981).
- U.S. EPA, Chromium(III), Integrated Risk Information System (IRIS), (1998a).
- U.S. EPA, Chromium(VI), Integrated Risk Information System (IRIS), (1998b).
- Weast, R.C., Astle, M. J., Beyer, W.H., eds. CRC Handbook of Chemistry and Physics, 69th edition (1988-1989), Chemical Rubber Company, Boca Raton.
- Wittbrodt, P. R., Palmer, C. D., Reduction of Cr(VI) in the presence of Excess
 Soil Fulvic Acid. Environ. Sci. Technol., 29(1995)255.
- Wozniak, D., Huang, J. Y. C., J. Water Pollution Control, 54(1982)1574.
- Yang, R. T., Gas Seperation by Adsorption Processes. Series on Chemical Engineering, vol. 1, Imperial College Press (1999).

APPENDIX A Tabular Results of Batch and Continuous Experiments

Initial Cr(VI) concentration (mg/l)	Solution phase Cr(VI) concentration at equilibrium (mg/l)	Solid phase Cr(VI) concentration at equilibrium (mg/g adsorbent)
20	1.854	1.452
40	5.140	2.788
60	13.50	3.720
80	24.00	4.480
100	37.50	5.000
150	75.00	6.000
200	106.0	7.520
250	145.0	8.400
300	186.0	9.120
400	259.0	11.27
500	343.0	12.50
800	622.0	14.19
1000	816.0	14.65
1200	1010	15.16
2000	1802	15.83

Table A1: Batch experiment results for adsorption isotherm of chromium (VI) and activated carbon system

Initial Cr(VI) ion concentration (mg/l)	Solution phase Cr(VI) concentration at equilibrium (mg/l)	Solid phase Cr(VI) concentration at equilibrium (mg/g adsorbent)
10	8	0.16
20	16	0.32
40	29	0.88
60	44	1.28
80	62	1.42
100	76	1.88
150	117	2.64
200	160	3.16
250	204	3.68
300	251	3.92
500	443	4.56

Table A2: Batch experiment results for adsorption isotherm of chromium (VI) and activated alumina system

Time (hours)	Effluent Cr(VI) concentration ratio (C/Co)
0	0
0.5	0
1	0.045
1.5	0.291
1.75	0.428
2	0.533
2.25	0.588
2.5	0.632
2.75	0.646
3	0.661
3.5	0.692
4.5	0.711
5.5	0.723
7	0.733
9	0.756
11	0.783
13	0.802
15	0.814
17	0.830
23	0.865
25	0.872

Table A3: Continuous experiment results for mass of Activated Carbon = 15 gm, inlet chromium(VI) concentration = 100 mg/l, flow rate = 15 ml/min, and particle size = 0.115 cm.

Time (hours)	Effluent Cr(VI)
	concentration ratio (C/Co)
0	0
1.5	0
1.75	0.006
2	0.068
2.25	0.177
2.75	0.420
3	0.512
3.25	0.551
3.5	0.578
3.75	0.597
4.25	0.612
5	0.631
6	0.661
8	0.680
10	0.705
12	0.721
14	0.742
16	0.765
18	0.783
22	0.801
24	0.811

Table A4: Continuous experimental results for mass of activated carbon = 15 gm, inlet chromium (VI) concentration = 100 mg/l, flow rate = 10 ml/min, and particle size = 0.115 cm.

Time (hours)	Effluent Cr(VI)
	concentration ratio (C/Co)
0	0
3.75	0
4.25	0.009
4.75	0.092
5	0.192
5.25	0.308
5.5	0.427
5.75	0.498
6	0.543
6.5	0.582
7	0.612
9	0.635
11	0.655
13	0.678
17	0.712
21	0.744
25	0.775

Table A5: Continuous experimental results for mass of activated carbon = 15 gm, inlet chromium (VI) concentration = 100 mg/l, flow rate = 5 ml/min, and particle size = 0.115 cm.

Time (hours)	Effluent Cr(VI) concentration ratio (C/Co)
0	0
1.5	0
2	0.005
2.5	0.081
2.75	0.145
3	0.210
3.25	0.297
3.5	0.366
3.75	0.422
4	0.469
4.5	0.542
5	0.577
5.5	0.602
7	0.631
9	0.682
11	0.711
13	0.733
15	0.762
17	0.783
19	0.802
21	0.823
25	0.844

Table A6: Continuous experiment results for mass of Activated Carbon in the bed = 15 gm, inlet chromium (VI) concentration = 50 mg/l, flow rate = 15 ml/min, and particle size = 0.115 cm.

Time (hours)	Effluent Cr(VI) concentration ratio (C/Co)
0	0
1	0
1.25	0.014
1.5	0.083
1.75	0.165
2	0.262
2.25	0.372
2.5	0.448
2.75	0.526
3	0.594
3.5	0.676
4	0.697
5	0.710
7	0.763
9	0.771
11	0.783
13	0.815
15	0.830
17	0.847
19	0.861
21	0.867
23	0.873

Table A7: Continuous experiment results for mass of Activated Carbon in the bed = 10 gm, inlet chromium (VI) concentration = 50 mg/l, flow rate = 15 ml/min, and particle size = 0.115 cm.

Time (hours)	Effluent Cr(VI) ion concentration ratio (C/Co)
0	0
2	0.007
2.75	0.329
3	0.433
3.33	0.495
3.66	0.562
4	0.599
4.5	0.638
5	0.650
6	0.676
7	0.684
9	0.720
11	0.748
13	0.772
15	0.778
21	0.829
24	0.845

Table A8: Continuous experimental results for mass of regenerated activated carbon = 15 g, inlet chromium (VI) concentration = 100 mg/l, flow rate = 5 ml/min, and particle size = 0.115 cm.

Time (hours)	Effluent Cr(VI) ion concentration ratio (C/Co)
0	
	0
1	0
1.5	0.136
1.75	0.562
2	0.637
2.25	0.663
2.5	0.676
2.75	0.687
3	0.690
3.5	0.700
6	0.729
8	0.756
10	0.783
12	0.807
14	0.823
16	0.837
18	0.852
20	0.864
22	0.882
24	0.902

Table A9: Continuous experimental results for mass of activated carbon = 15 g, inlet chromium (VI) concentration = 100 mg/l, flow rate = 15 ml/min, and particle size = 0.0445 cm.

Effluent Cr(VI) ion concentration ratio (C/Co)
0
0.067
0.140
0.243
0.330
0.429
0.561
0.620
0.673
0.718
0.771
0.800
0.843
0.856
0.875
0.898
0.929
0.947

Table A10: Continuous experimental results for mass of activated carbon = 15 g, inlet chromium (VI) concentration = 100 mg/l, flow rate = 15 ml/min, particle size = 0.198 cm.

APPENDIX B

Model Parameters and Constants

Diameter of column = D = 1.4 cm

Density of the bed = $\rho = 0.38$ g/cc

Porosity of the bed = $\varepsilon = 0.45$

Internal porosity of the adsorbent particle = X = 0.67

Diffusivity of chromium(VI) ion in water = $D_1 = 4.31*10^{-5}$ cm²/sec

Kinematic viscosity of water = $v = 8.64*10^{-3} \text{ cm}^2/\text{sec}$

Density of activated carbon (adsorbent) = 1.3 g/cm^3

APPENDIX C Code in C Language for the Model

```
#include<stdio.h>
#include<math h>
main()
{
int t,i,n,i,z;
double area,dl,c,a,b,u,X,visco,delt,rhop,r;
double epsi, v, k, czero, mass, rho, d, dp, volu, l, kpap, kfap, nre, jd, ap, kf.
double c1[25],c2[25];
double q1[25],q2[25];
/*.....*/
/*mass of adsorbent in the fixed bed in g and flow rate of water in cc/sec*/
/*inlet fluoride ion concentration in mg/l and elapsed time in seconds*/
/*particle size in cm*/
printf("enter mass,flow rate,inlet conc, particle size, number of elements for model and
time\n");
scanf("%lf%lf%lf%lf%\d%d",&mass,&u,&czero,&dp,&n,&t);
/*.....*/
             /*column diameter in, cm*/
d=1.4;
rhop=1.3; /* density of adsorbent particle in gm/cm<sup>3</sup>*/
rho=0.38; /*bed density in, g/cc*/
dl=4.31e-5; /*diffusivity of fluoride ion in water in, cm<sup>2</sup>/sec*/
epsi=0.45; /*bed porosity dimension less*/
            /*internal porosity of adsorbent particle dimension less*/
X=0.67;
visco=8.64e-3; /*kinematic viscosity of solution in cm²/sec*/
area=3.141*d*d/4; /*cross-sectional area of column in, cm<sup>2</sup>*/
                 /*volume of the bed in cm<sup>3</sup>*/
volu=mass/rho:
             /*length of the bed in, cm*/
l=volu/area:
```

```
v=volu/n;
             /*volume of each element*/
ap=(6/dp)*rhop; /*external interfcial transfer area of adsorbent in, cm<sup>2</sup>/cm<sup>3</sup>*/
/*.......Calculation of Pore Diffusion Mass Transfer Coefficient......*/
kpap=(30.0*d1*X)*(1-epsi)/(dp*dp); /* in per sec*/
/*......Calculation of External Film Diffusion Mass Transfer Coefficinet......*/
nre=(u*dp)/((1-epsi)*area*visco); /*Reynolds number*/
id=5.7*(pow(nre,-0.78));
                                   /*mass transfer factor id*/
kf=jd*u*(pow((dl/visco),0.66))/area; /*external mass transfer coefficient in cm/sec*/
kfap=kf*ap; /* external mass transfer coefficient in per sec*/
/*....Calculation of over-all Mass Transfer Coefficent...*/
k=1/((1/kpap)+(1/kfap)); /* overall mass transfer coefficient in per sec*/
                        /* constant with dimension in per sec*/
e=(u/(epsi*v));
f=(rho/(epsi*rhop))*k; /* constant with dimension in per sec*/
                       /* time interval in sec*/
delt=0.5/(a+b);
r=1/0.101:
/*.......Initial Conditions for Solution and Solid Phase Concentration......*/
 for(z=1;z\leq n;z++)
c1[z]=0.0; /*solution phase initial concentration for all elements in, mg/l*/
q1[z]=0.0; /*solid phase initial concentration for all elements in, mg/g*/
}
for(i=0;i<=j;i++)
{
c1[0]=czero; /*inlet solution phase chromium ion concentration in, mg/l*/
 }
/*Calculation of Solution and Solid phase Concentration for any Element at any
Time*/
i=t/delt;
for(i=1;i<=i;i++)
 {
for(z=1;z<=n;z++)
```

```
{
    /*solid phase fluoride ion concentration*/
    q2[z]=q1[z]+((delt*0.001*k)/rhop)*(c1[z]-q1[z]*r);

/*solution phase fluoride ion concentration*/
    c2[z]=c1[z]+e*delt*(c1[z-1]-c1[z])-f*delt*(c1[z]-q1[z]*r);
    c1[z]=c2[z];
    q1[z]=q2[z];
}

/*...Printing of Solution Phase Concentration ratio for each Element at any Time..*/
for(z=1;z<=n;z++)
{
    printf("\n c1[%d]=%f",z,c1[z]/czero);
}
}
```